Study of magneto-electric coupling between ultra-thin Fe films and PMN-PT using X-ray magnetic circular dichroism

S. R. V. Avula, J. Heidler, J. Dreiser, J. Vijayakumar, L. Howald, F. Nolting, and C. Piamonteze[a)]
Swiss Light Source, Paul Scherrer Institut, 5232 Villigen PSI, Switzerland

(Received 30 August 2017; accepted 20 January 2018; published online 12 February 2018)

X-ray absorption spectra and magnetic circular dichroism were measured at the Fe $L_{3,2}$-edges of an iron wedge deposited on a ferroelectric substrate in the total electron yield mode. Upon switching the ferroelectric polarization from P_{up} to P_{down}, we observe a relative change in the total magnetic moment of 20% for 1.5 nm thin Fe. For 3 nm thin Fe, the relative change is within the sum rule error bar. Taking the sampling depth of the measurement method into account, this difference is compatible with a magnetic anisotropy change taking place in the first interfacial layer in contact with the ferroelectric substrate. We attribute this interfacial coupling to a charge accumulation or depletion at the interface. https://doi.org/10.1063/1.5002530

I. INTRODUCTION

Artificial multiferroic materials are heterostructures where ferromagnetic (FM) and ferroelectric (FE) materials are magneto-electrically (ME) coupled.[1,2] These systems are of great interest for developing new functional devices. Manipulating magnetism with the electric field is very appealing for applications in low power consumption devices.[3] The study of the coupling mechanisms at the interface is therefore of importance in order to achieve better multiferroics. The interfacial coupling can be grouped into three main mechanisms, such as coupling through strain,[4–6] coupling through charge modulation,[7] and coupling by exchange bias.[8] Recently, the co-existence of strain and charge mechanisms in artificial multiferroic systems at room temperature has been shown.[9–12] The magneto-electric coupling by charge modulation, which we address in this work, can lead to various effects in the system. In magneto-electrically coupled $Pb(Zr_{0.2}Ti_{0.8})O_3/La_{0.8}Sr_{0.2}MnO_3$, it has been shown that charge modulation at the interface leads to a change of the valence state of Mn.[13] More recently, it was shown that the coercive field in $CoFeB/BaTiO_3$ can be modulated using the FE polarization of $BaTiO_3$.[14] Other observations are the change of the magnetic properties of ultra-thin Fe films in Fe/MgO tunnel junctions[15] and change of the tunnel magnetoresistance of $Fe/BaTiO_3/LaSrMnO_3$ junctions.[16]

First principles calculations on $Fe/BaTiO_3$ predict the characteristic features in X-ray magnetic circular dichroism (XMCD) and change in the magnetic order with the increasing Fe-film thickness from 1 to 3 monolayers (ML).[17,18] XMCD experiments agree with the theoretical calculations for 2 ML of Fe grown on $BaTiO_3$ thin films.[19] In this work, we study the magneto-electric coupling between an ultra-thin Fe film and ferroelectric substrate $Pb[(Mg_{1/3}Nb_{2/3})O_3]_{(1-x)}$-$[PbTiO_3]_x$, $x = 0.32$ (PMN-PT). We have employed XMCD to quantitatively analyse the total magnetic moment of Fe. Upon switching the FE polarization, we observe a change of about 20% of total magnetic moment of Fe for 1.5 nm thin Fe films, while the change for the 3 nm thin Fe film is within the sum rule error bar. Using an expression for the X-ray absorption spectra (XAS) taking into account the probing depth,[20] we can model this thickness dependence. We show that our results agree with a change in magnetic moment only in the first interfacial layer of Fe in contact with the FE substrate. We attribute the origin of the magneto-electric coupling observed to charge modulation at the interface between Fe and PMN-PT.

II. EXPERIMENTAL

Relaxor (001)-oriented PMN-PT (Atom Optics Co. LTD) was chosen as the FE substrate,[21] due to strong FE polarization. First, a bottom contact of a 30 nm thick Au layer was deposited on the back of the PMN-PT for the switching of the FE polarization. Next, the substrate was introduced in a UHV sample preparation chamber. Inside this chamber, the substrate was heated to 110 °C for 30 min to remove the water from the surface. A continuous wedge of Fe with the thickness varying from 0.3 nm to 3 nm was grown on PMN-PT using an electron-beam evaporator under ultra-high vacuum ($\sim 10^{-9}$ mbar) conditions with the substrate held at room temperature. A 3 nm thick Cr film was grown on top of Fe to provide a continuous conductive layer acting as a top electrode. The FE polarization was switched in the beamline's sample preparation chamber by ramping the electric field between +/− 2.2 kV/cm, and the I-V curve was recorded to confirm the switching. In this paper, we use the terms P_{up} and P_{down} for the FE polarization direction as shown in Fig. 1. The sample preparation chamber is connected to the measuring chamber, and the sample is transferred under ultra-high vacuum conditions. The XAS and XMCD experiments were carried out at the X-Treme

a)Email: cinthia.piamonteze@psi.ch

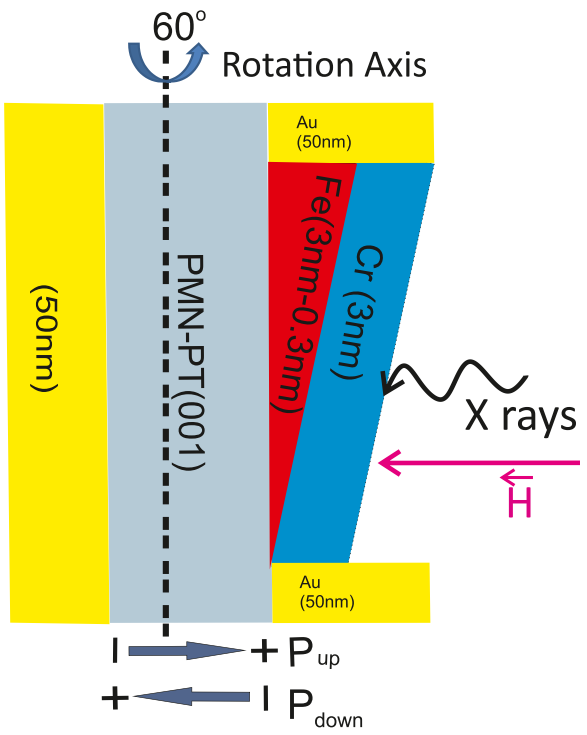

FIG. 1. Schematic of the investigated sample with the marked direction of the FE polarization vector. The X-rays impinge on the sample at grazing or normal incidence.

beamline at the Swiss Light Source.[22] The XAS and XMCD spectra were acquired in the total electron yield (TEY) mode and without the applied electric field to avoid unnecessary noise. Due to the high electric susceptibility of PMN-PT, the polarization remains unaffected throughout the measurements. The measurements were performed at a base temperature of ∼1.5 K at the cold finger which corresponds to 2.0–3.0 K at the sample. Data were taken at nominal Fe thicknesses of 0.3 nm, 1.5 nm, and 3 nm film which correspond to 1 ML, 5 ML, and 10 ML,[23] respectively. The absorption spectra were recorded at Fe $L_{3,2}$ -edges in two geometries: with X-rays at an angle of 60° to the surface normal (i.e., 30° of grazing incidence) and parallel to the surface normal (normal incidence) (see Fig. 1). The XMCD measurements were first taken in an applied magnetic field of 6.8 T and then in remanence. The XAS spectra plotted are the sum of the spectra measured with X-ray right ($c+$) and left ($c-$) circular polarization of the X-rays and the XMCD is defined as ($c+$ - $c-$).

III. RESULTS AND DISCUSSION

The magnetization direction of the Fe film was probed by measuring the XMCD signal at grazing and normal incidence at different Fe film thicknesses. As the saturation field for 0.3 nm thin Fe was unknown, we applied the maximum field available of 6.8 T. A field of 0.5 T was enough to saturate the 1.5 nm thin Fe. The saturation field was determined by measuring a hysteresis curve using XMCD on a test sample along grazing incidence at 3 K, consisting of 1.5 nm thin Fe deposited on PMN-PT (011). No remanent magnetization was detected for 0.3 nm thin Fe, while a clear in-plane magnetization was observed for 1.5 nm Fe, shown in Fig. 2(b) and for 3 nm Fe (not shown). The small XMCD observed at normal incidence of the film shown in Fig. 2(a) is attributed to the small remanence of the superconducting magnet coils of about 5 mT.[22]

In order to study the effect on the Fe magnetization due to the PMN-PT FE polarization, XMCD measurements were performed with FE polarization P_{up} and P_{down} (see Fig. 1). The data are shown in Figs. 3(a)–3(c) for the applied magnetic field and in Figs. 3(d)–3(f) in remanence, for 0.3 nm, 1.5 nm, and 3 nm thin Fe, respectively. No change in XMCD is observed for measurements in the applied magnetic field for the aforesaid thicknesses of Fe. No remanence was observed for 0.3 nm thin Fe for both FE polarizations as shown in Fig. 3(d). As we do not observe

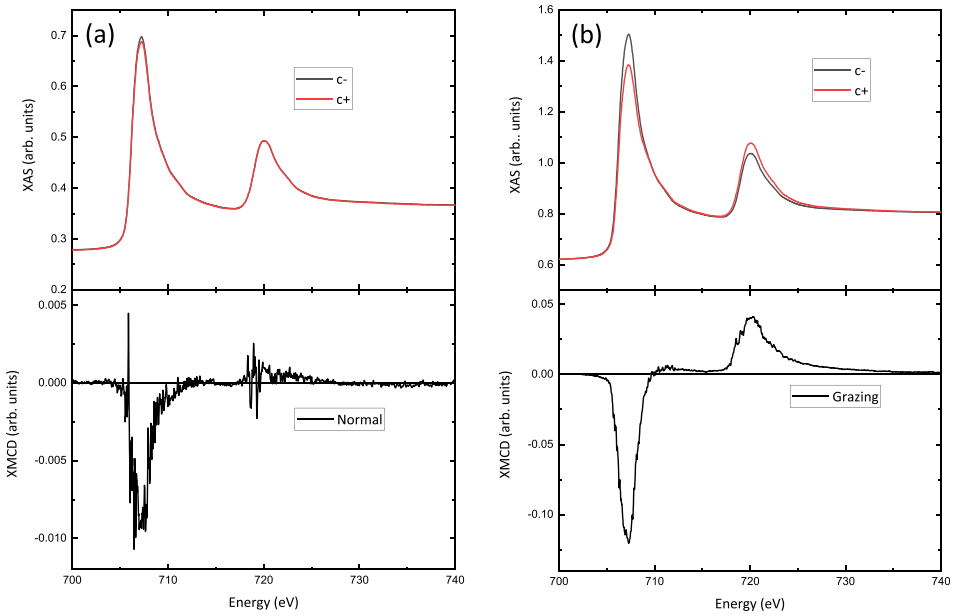

FIG. 2. The XAS and XMCD measured at $L_{3,2}$ edges at 1.5 nm thin Fe in remanence at 3 K (a) at normal incidence and (b) at 60° to the surface normal.

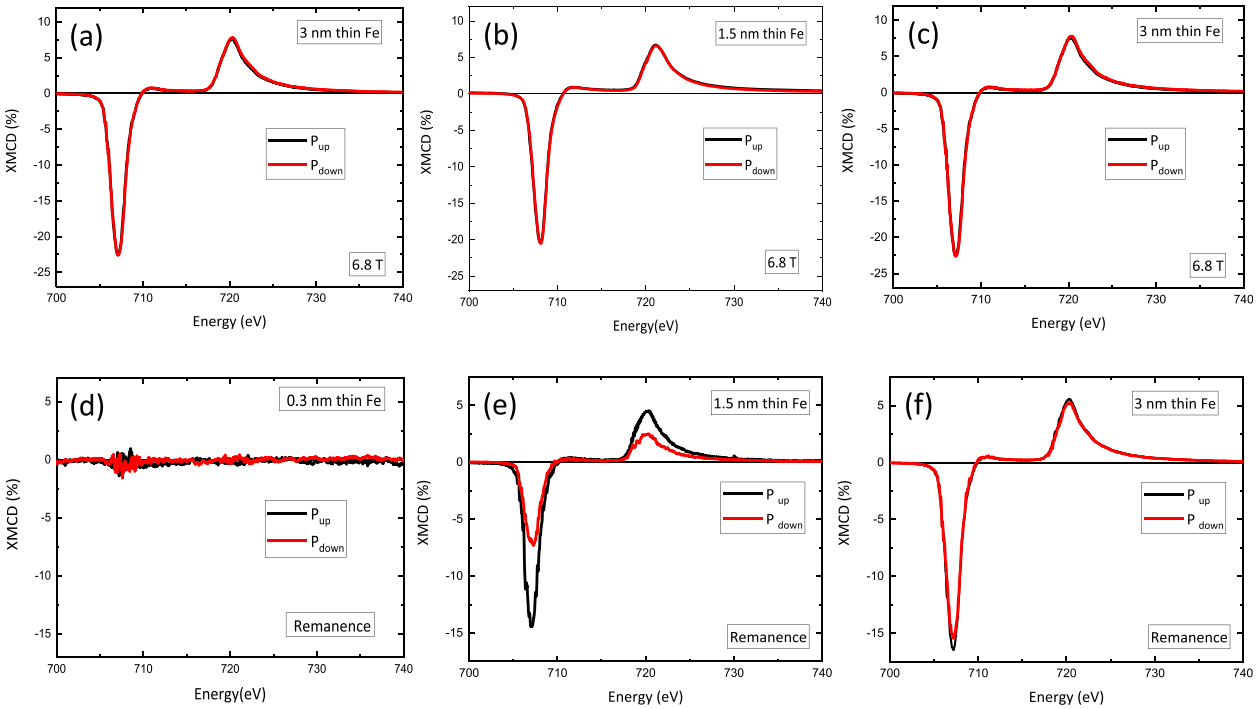

FIG. 3. XMCD measured at Fe $L_{3,2}$ edges for 0.3 nm (a), 1.5 nm (b), and 3 nm (c) thin Fe in saturation at 6.8 T, and 0.3 nm (d), 1.5 nm (e), and 3 nm (f) in remanence for both FE polarizations at 3 K. The measurements were performed at 60° to the surface normal.

any oxidation at the Fe $L_{3,\ 2}$ edges [see Fig. 4(a)], we believe that the ultra-thin Fe film does not show remanence because it grows in the form of nano-islands which will be superparamagnetic at 3 K. This Fe nanoisland growth has been observed by Radaelli *et al.*[19] for Fe on $BaTiO_3$. Their TEM results show that Fe grows in the form of nanoislands in the thickness range of 1–4 ML. A clear change for the XMCD measured in remanence was observed for the 1.5 nm thin Fe film. As shown in Fig. 3(e), for the 1.5 nm thin Fe film, the XMCD in remanence is nearly 14% of the Fe L_3 XAS for P_{up} polarization and decreases to 8% for P_{down}. For the 3 nm thin Fe film, a much smaller change in XMCD between P_{up} and P_{down}, of about 1% of the Fe L_3 XAS, is observed [see Fig. 3(f)].

Figures 4(a)–4(c) show the XAS for both FE polarizations of PMN-PT measured for 0.3 nm, 1.5 nm, and 3 nm thin Fe. For the whole thickness range along the wedge, the XAS measured for Fe agrees with a metallic valence state. Comparing different FE polarization directions, no change in the XAS shape is observed. Our results are therefore different from what was previously observed in the Fe/MgO/Fe interface,[24] where a clear oxidation of Fe is observed. At the Fe/BTO interface,[19] an additional peak in the Fe L_3- edge is observed and is attributed to the Fe-O hybridization.

The Fe spin and orbital magnetic moments obtained from the XMCD sum rules[25,26] are presented in Table I. The number of 3d electrons used for Fe was 6.61.[27] For the 0.3 nm thin Fe, we find very small moments in the applied magnetic field. Even for 1.5 nm thin Fe, the total remanent moment is much smaller than 2.06 μ_B, which was previously measured for thicker Fe films.[27] We believe that this difference comes from the fact that Fe grows initially in islands which are not connected for the smallest thicknesses. For 1.5 nm thin Fe in remanence, the moment decreases from 0.90(8) μ_B to 0.71(8) μ_B by switching FE polarization from P_{up} to P_{down}. For the 3 nm thin Fe film, a small change is visible in the XMCD spectra [Fig. 3(f)]; however, the calculated change in the magnetic moment from 1.90(5) μ_B to 1.85(8)

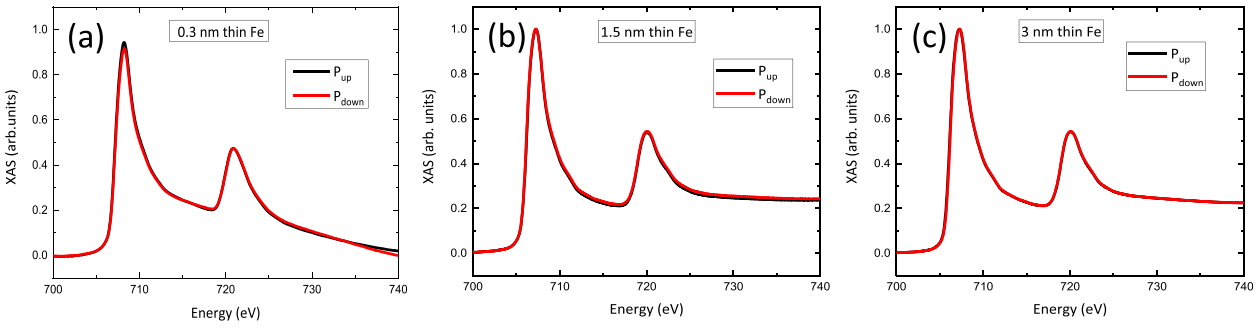

FIG. 4. XAS measured at Fe $L_{3,2}$ edges for 0.3 nm (a), 1.5 nm (b), and 3 nm (c) for both FE polarizations at 3 K in remanence at grazing incidence of the X-rays.

TABLE I. The effective spin moment ($M_{s,eff}$), orbital moment (M_l), and total magnetic moment ($M_{tot.}$), per atom of Fe for 0.3 nm, 1.5 nm, and 3 nm thin Fe in remanence and applied field for both FE polarizations along grazing incidence and at 3 K.

Fe nominal thickness (nm)	FE polarization	Applied field (T)	M_l (μ_B)	$M_{s,eff}$ (μ_B)	$M_{tot.}$(μ_B)
0.3	P_{up}	6.8	0.03(3)	0.30(6)	0.33(6)
	P_{down}		0.02(4)	0.28(4)	0.30(5)
1.5	P_{up}	0.0	0.06(5)	0.84(8)	0.90(8)
	P_{down}		0.03(5)	0.68(7)	0.71(8)
	P_{up}	6.8	0.08(4)	1.80(6)	1.88(7)
	P_{down}		0.07(5)	1.77(4)	1.84(6)
3	P_{up}	0.0	0.15(5)	1.75(3)	1.90(5)
	P_{down}		0.14(5)	1.71(7)	1.85(8)
	P_{up}	6.8	0.17(4)	1.93(2)	2.10(4)
	P_{down}		0.15(6)	1.90(3)	2.05(6)

μ_B is within the error bar. The saturation moments for 1.5 nm and 3 nm for both FE polarizations are also shown in Table I.

As observed from the sum rule results, there is a large change in the Fe remanent magnetic moment for 1.5 nm thin Fe with FE polarization switching, while only a minor change is observed for 3 nm thin Fe. In the following discussion, we would like to address this difference in total magnetic moment for 1.5 nm and 3 nm thin Fe. As mentioned previously, we employed the TEY detection mode to measure the XMCD. This mode measures the drain current which is created to replace the electrons leaving the sample due to the X-ray absorption. Since the probability for an electron to leave the sample decays with the distance from the surface, top layers (TLs) contribute more to the total signal than deeper layers far from the surface.[28] Therefore, the probability for an electron to escape from the Fe/PMN-PT interface decays exponentially with the increasing Fe top layer thickness. The measured electron escape depth λ is 1.75 nm for Fe.[29] Consequently, due to the higher sensitivity to the top surface in the TEY detection mode, the interface contribution to the total signal will be higher for the 1.5 nm thin Fe compared to the 3 nm thin Fe. In the following, we use the derivation from Regan *et al.*[20] to test if the observed difference in the sum rule results with FE polarization switching fits to the probing depth of TEY.

By taking into account the limited probing depth, Regan *et al.*[20] derived expressions for the total XAS signal ($N(E)^{\text{Total}}$) measured by TEY, where E is the photon energy. We separate the total signal into the contribution of the top layers (TLs), not affected by charge accumulation/depletion and the interfacial layer where charge accumulation/depletion may occur. Since the charge screening length of Fe is 0.13 nm,[30] we assume here that the interface layer (IL) is 0.3 nm thin, which corresponds to 1 ML. So, the total XAS signal is

$$N(E)^{\text{Total}} = N(E)^{\text{TL}} + N(E)^{\text{IL}}. \tag{1}$$

The expression used to calculate the XAS signal from the top layer is given by

$$N(E)^{\text{TL}} = \text{I}_\text{o}\,\lambda G(E)\mu(E)\left(1 - \text{e}^{-t_{\text{TL}}/\lambda}\right). \tag{2}$$

Here, I_o is the number of incident photons on the sample, $G(E)$ is the number of electrons produced per photon, and t_{TL} is the thickness of the TL. In Eq. (2), we have used the expression derived by Regan *et al.*[20] for the unsaturated TEY signal since λ is much smaller than the X-ray penetration length given by $1/\mu(E)$, where $\mu(E)$ is the absorption coefficient and it varies between 0.5 μm and 0.04 μm for the Fe energy ranging from 690 eV to 750 eV. The following expression was used to calculate the XAS signal from the interfacial layer:

$$N(E)^{\text{IL}} = \text{I}_o G(E)\mu(E)t_{\text{IL}}\left(1 - \frac{t_{\text{IL}}}{2\lambda}\right)\text{e}^{-t_{\text{TL}}/\lambda}. \tag{3}$$

In the above expression, t_{IL} is the thickness of the IL. Equation (3) for the IL was obtained by expanding the exponential term in Eq. (2) up to second order. This is justified since t_{IL} is approximately 0.3 nm which is much smaller than $\lambda = 1.75$ nm. Moreover, the XAS signal from the IL is further attenuated by a factor of $e^{-t_{TL}/\lambda}$ representing the effect from the TL. For 1.5 nm and 3 nm thicknesses of Fe, the TL thickness is 1.2 nm and 2.7 nm, respectively. Using these values for t_{TL} and t_{IL} in the above expressions, we obtain that the relative contribution of the IL signal to the total signal is 12% and 4% for 1.5 nm and 3 nm thin Fe, respectively.

The total magnetic moment can also be divided into a contribution from the TL and the IL as

$$M^{\text{Total}} = \frac{Z}{Z+1}M^{\text{TL}} + \frac{1}{Z+1}M^{\text{IL}}, \tag{4}$$

where $z = \frac{N(E)^{\text{TL}}}{N(E)^{\text{IL}}}$.

In expression (4), M^{TL} and M^{IL} are the magnetic moments of the TL and the IL, respectively. The total observed change in XMCD with the ferroelectric polarization from P_{up} to P_{down} (ΔM^{Total}), i.e., $\Delta M^{\text{Total}} = M^{\text{Total}}_{\text{Pup}} - M^{\text{Total}}_{\text{Pdown}}$, can be written in terms of change in the magnetic moment of the top layer (ΔM^{TL}) and the interfacial layer (ΔM^{IL}) with ferroelectric polarization

$$\Delta M^{\text{Total}} = \frac{Z}{Z+1}\Delta M^{\text{TL}} + \frac{1}{Z+1}\Delta M^{\text{IL}}. \tag{5}$$

Our model assumes that the change in the total magnetic moment comes from the IL only and not from the TL. Therefore, ΔM^{TL} is zero and the expression above reduces to

$$\Delta M^{\text{Total}} = \frac{1}{Z+1}\Delta M^{\text{IL}}. \tag{6}$$

Using Eqs. (2) and (3), we obtain $Z \sim 7$ for 1.5 nm and 24 for 3 nm. By using the measured ΔM^{Total} for 1.5 nm and $Z = 7$ in Eq. (6), we obtain $\Delta M^{\text{IL}} = 1.52\ \mu_B$. Since ΔM^{IL} is independent of the film thickness, we then obtain $\Delta M^{\text{Total}} = 0.06\ \mu_B$ for the 3 nm thin Fe film. This total change of moment for 3 nm (0.06 μ_B) is comparable to the total change in magnetic moment we obtain from the sum rules (0.05 μ_B). Therefore, our initial hypothesis that the change in magnetic moment measured occurs only at the IL in contact with the FE is in agreement with these calculations. As the charge accumulation and depletion is an interfacial effect due to the charge

screening length of Fe, this infers that the magnetoelectric coupling observed is driven by charge modulation at the Fe/PMN-PT interface.

IV. CONCLUSIONS

Fe/PMN-PT shows a magneto-electrical coupling. The magnetic moment of Fe decreases by switching the ferroelectric polarization of PMN-PT from P_{up} to P_{down}. Due to the difference in the thickness of the Fe and the same probing depth of X-rays, the measured moment change is larger for the thinner part of the wedge as compared to the thicker part. Our analysis shows that the Fe interface layer to PMN-PT is affected by the FE polarization and its moment changes by 1.50 μ_B. No change in the saturation moment but only in the remanent moment is observed, which is in agreement with a change in magnetic anisotropy. As the change in magnetic moment occurs at the interfacial layer, we attribute this effect to charge accumulation and depletion at the Fe/PMN-PT interface.

ACKNOWLEDGMENTS

We acknowledge financial support from the Swiss National Science Foundation (Grant No. 200021_146715 and J.V was supported by Grant No. 200021_153540). The X-ray absorption measurements were performed on the EPFL/PSI X-Treme beamline at the Swiss Light Source, Paul Scherrer Institut, Switzerland. We thank Stefan Zeugin for technical support.

[1]N. A. Spaldin and M. Fiebig, Science **309**, 391 (2005).
[2]R. Ramesh and N. A. Spaldin, Nat. Mater. **6**, 21 (2007).
[3]C. A. Fernandes Vaz and U. Staub, J. Mater. Chem. C **1**, 6731 (2013).
[4]C. Thiele, K. Dörr, O. Bilani, J. Rödel, and L. Schultz, Phys. Rev. B **75**, 054408 (2007).
[5]M. Weiler, A. Brandlmaier, S. Geprägs, M. Althammer, M. Opel, C. Bihler, H. Huebl, M. S. Brandt, R. Gross, and S. T. B. Goennenwein, New J. Phys. **11**, 013021 (2009).
[6]R. V. Chopdekar, V. K. Malik, A. Fraile Rodríguez, L. Le Guyader, Y. Takamura, A. Scholl, D. Stender, C. W. Schneider, C. Bernhard, F. Nolting, and L. J. Heyderman, Phys. Rev. B **86**, 014408 (2012).
[7]H. J. A. Molegraaf, J. Hoffman, C. A. F. Vaz, S. Gariglio, D. Van Der Morel, C. H. Ahn, and J. M. Triscone, Adv. Mater. **21**, 3470 (2009).
[8]V. Skumryev, V. Laukhin, I. Fina, X. Martí, F. Sánchez, M. Gospodinov, and J. Fontcuberta, Phys. Rev. Lett. **106**, 057206 (2011).
[9]L. Shu, Z. Li, J. Ma, Y. Gao, L. Gu, Y. Shen, Y. Lin, and C. W. Nan, Appl. Phys. Lett. **100**, 022405 (2012).
[10]J. M. Hu, C. W. Nan, and L. Q. Chen, Phys. Rev. B **83**, 134408 (2011).
[11]T. Nan, M. Liu, W. Ren, Z.-G. Ye, and N. X. Sun, Sci. Rep. **4**, 5931 (2014).
[12]J. Heidler, M. Fechner, R. V. Chopdekar, C. Piamonteze, J. Dreiser, C. A. Jenkins, E. Arenholz, S. Rusponi, H. Brune, N. A. Spaldin, and F. Nolting, Phys. Rev. B **94**, 014401 (2016).
[13]C. A. F. Vaz, J. Hoffman, Y. Segal, J. W. Reiner, R. D. Grober, Z. Zhang, C. H. Ahn, and F. J. Walker, Phys. Rev. Lett. **104**, 127202 (2010).
[14]L. Baldrati, C. Rinaldi, A. Manuzzi, M. Asa, L. Aballe, M. Foerster, N. Biškup, M. Varela, M. Cantoni, and R. Bertacco, Adv. Electron. Mater. **2**, 1600085 (2016).
[15]T. Maruyama, Y. Shiota, T. Nozaki, K. Ohta, N. Toda, M. Mizuguchi, A. A. Tulapurkar, T. Shinjo, M. Shiraishi, S. Mizukami, Y. Ando, and Y. Suzuki, Nat. Nanotechnol. **4**, 158 (2009).
[16]S. Valencia, A. Crassous, L. Bocher, V. Garcia, X. Moya, R. O. Cherifi, C. Deranlot, K. Bouzehouane, S. Fusil, A. Zobelli, A. Gloter, N. D. Mathur, A. Gaupp, R. Abrudan, F. Radu, A. Barthélémy, and M. Bibes, Nat. Mater. **10**, 753 (2011).
[17]M. Fechner, I. V. Maznichenko, S. Ostanin, A. Ernst, J. Henk, P. Bruno, and I. Mertig, Phys. Rev. B **78**, 212406 (2008).
[18]S. Borek, I. Maznichenko, G. Fischer, W. Hergert, I. Mertig, A. Ernst, S. Ostanin, and A. Chassé, Phys. Rev. B **85**, 134432 (2012).
[19]G. Radaelli, D. Petti, E. Plekhanov, I. Fina, P. Torelli, B. R. Salles, M. Cantoni, C. Rinaldi, D. Gutiérrez, G. Panaccione, M. Varela, S. Picozzi, J. Fontcuberta, and R. Bertacco, Nat. Commun. **5**, 3404 (2014).
[20]T. J. Regan, H. Ohldag, C. Stamm, F. Nolting, J. Lüning, J. Stöhr, and R. L. White, Phys. Rev. B **64**, 214422 (2001).
[21]J. Luo and S. Zhang, Crystals **4**, 306 (2014).
[22]C. Piamonteze, U. Flechsig, S. Rusponi, J. Dreiser, J. Heidler, M. Schmidt, R. Wetter, M. Calvi, T. Schmidt, H. Pruchova, J. Krempasky, C. Quitmann, H. Brune, and F. Nolting, J. Synchrotron Radiat. **19**, 661 (2012).
[23]J. Vogel, A. Fontaine, V. Cros, F. Petroff, J.-P. Kappler, G. Krill, A. Rogalev, and J. Goulon, J. Magn. Magn. Mater. **165**, 96 (1997).
[24]S. Gautam, K. Asokan, J. P. Singh, F. Chang, H. Lin, and K. Hwa, J. Appl. Phys. **115**, 17C109 (2014).
[25]B. T. Thole, P. Carra, F. Sette, and G. Van Der Laan, Phys. Rev. Lett. **68**, 1943 (1992).
[26]P. Carra and M. Altarelli, Phys. Rev. Lett. **70**, 694 (1993).
[27]C. Chen, Y. Idzerda, H.-J. Lin, N. Smith, G. Meigs, E. Chaban, G. Ho, E. Pellegrin, and F. Sette, Phys. Rev. Lett. **75**, 152 (1995).
[28]C. J. Powell, Surf. Sci. **44**, 29 (1974).
[29]R. Nakajima, J. Stöhr, and Y. Idzerda, Phys. Rev. B **59**, 6421 (1999).
[30]S. Zhang, Phys. Rev. Lett. **83**, 640 (1999).